J. Membrane Biol. 121, 189–198 (1991)
0022263191000663

The Journal of
Membrane Biology

Ion Channels in Murine Nuclei during Early Development and in Fully Differentiated Adult Cells

M. Mazzanti*, L.J. DeFelice, and E.F. Smith
Department of Anatomy and Cell Biology, Emory University School of Medicine, Atlanta, Georgia 30322

Summary. The nuclear envelope functions as a selective barrier between nucleus and cytoplasm. During cycles of cell division the nuclear envelope repeatedly disassembles and re-associates. Presumably, each cycle re-establishes the functional and structural integrity of the nuclear envelope. After repeated rounds of cell division, as occurs during differentiation, the selectivity and configuration of the envelope may change. We compare the ionic conductance and the nuclear pore density in four types of murine nuclei: germinal vesicles in oocytes, pronuclei in zygotes, nuclei from two-cell blastomeres, and somatic cell nuclei from the liver. A large-conductance ion channel is present in all nuclear envelopes. Liver cell nuclei have a greater number of these channels than those from earlier developmental stages, and they also have a higher density of nuclear pores. In this article we hypothesize an association between the ion channels and the nuclear pores.

Key Words nuclear envelope · ion channels · patch clamp · nuclear pores · development

Introduction

Nuclear envelopes are composed of inner and outer membranes. Large pores span both of these membranes, and a fibrillar network, the nuclear lamina, underlies the inner membrane. During the normal cell cycle the nuclear envelope disassembles and reassociates, and its components regain both functional and structural integrity in each successive division. During interphase, for example, the nuclear envelope passes ions, proteins, nucleotides, and RNA from one side to the other (Dingwall & Laskey, 1986; Newport & Forbes, 1987; Gerace, 1988). The selectivity of the proteins and the RNA is attributed to the nuclear pores.

Because nuclear pores contain a large central canal approximately 90 Å in diameter (Unwin & Milligan, 1982; Akey, 1989), they are generally assumed to be freely permeable to water and ions. In some cells, however, an electrical potential exists between the nucleoplasm and the cytoplasm (Loewenstein & Kanno, 1963; Ito & Loewenstein, 1965; Mazzanti et al., 1990), indicating an unequal distribution of ions across the envelope. Although electrogenic pumps or ion-discriminating, nucleoplasmic absorption could maintain electrical potentials in the presence of large, nonselective pores, the presence of nuclear resting potentials is essentially counter to the free diffusion of ions across the envelope.

In a previous report we attributed the nuclear resting potential in the mouse pronucleus partly to the presence of 200-pS, K-selective channel in the nuclear membrane (Mazzanti et al., 1990). Although the chance of finding these channels in the 200-pS state was low (10%), we concluded that since it was the largest conductance, 200 pS corresponds to a fully open channel. We used a zygote enucleation procedure to obtain nuclei for these experiments because pronuclei recuperate from micromanipulation and the preparation is therefore functional. In the present article we compare the electrical properties of the pronucleus with three other nuclei: germinal vesicles from mouse oocytes, nuclei from two-cell embryos (both preparations by enucleation), and somatic cell nuclei from adult liver (by homogenization and centrifugation). The latter procedure is more convenient than enucleation, and it provides a larger number of nuclei. We investigate the ultrastructure of the nuclear envelope for each preparation. Our data suggest a correlation between the number of ion channels and the number of nuclear pores in the envelope.

* *Present address:* Fisiologia e Biochemica Generale, Università di Milano, via Celoria 26, 20133 Milan, Italy.

Materials and Methods

Preparation

We superovulated female B6D2 F_1 mice with 5 IU of PMSG (McGrath & Solter, 1983), which was followed in 48 hr by 5 IU HCG (Sigma). To obtain pronuclei or two-cell embryo stage nuclei, we mated females with B6D2 F_1 males. Eggs or zygotes were harvested approximately 12 hr after the injection or mating. Incubation in a 1% hyaluronidase solution for several minutes facilitated removal of cumulus cells from the eggs or the zygotes. After transferring the cells to the bath solution which contained (in mM): 120 KCl, 2 $MgCl_2$, 1.1 EGTA, 0.1 $CaCl_2$, 5 glucose, and 10 HEPES, pH 7.4, we extracted the nucleus using the micromanipulation technique of McGrath and Solter (1983).

Using the same breed of mice, we isolated liver nuclei by shearing fresh liver tissue in a homogenizer with a Teflon pestle of 0.025 μm clearance, and centrifuging the homogenate on a sucrose pad which contained (in mM): 50 Tris HCl, 25 KCl, 5 $MgCl_2$, and 250 sucrose at 30,000 rev/min in a Beckman SW41 rotor at 0–4°C (Blobel & Potter, 1966). This procedure results in a pellet of pure nuclei, which we resuspend in the standard bath solution before use.

Micromanipulation may leave plasma membrane or endoplasmic reticulum (ER) attached to the nucleus. In that case we could be patching these membranes rather than the nuclear envelope (*see* Discussion). The McGrath and Solter (1983) micromanipulation technique and the Blobel and Potter (1966) extraction procedure result in rather similar patches except for channel number (*see* Results), We therefore suppose that the patches are formed on the outer membrane of the nuclear envelope, free of extranuclear material; however, we cannot entirely eliminate other possibilities.

Single-Channel Recording

Patch electrodes were pulled from hard borosilicate glass (Corning 7052) on a Sachs-Flaming P-84 puller (Sutter Instruments). The pipettes were coated with Sylgard® (Dow Corning) and fire-polished to an external tip diameter of about 1 μm. These electrodes had resistances of 4–10 MΩ. The estimated surface area of the patch formed with these electrodes is 5–7 μm^2 (Mazzanti & DeFelice, 1987). We applied standard cell-attached patch-clamp techniques to obtain nucleus-attached patches and single-channel recordings from the four kinds of nuclei. In the single-channel experiments the preparations were bathed in the standard bath solution (*see* text). The patch pipette contained this same solution. Single-channel currents were recorded with a List EPC-7 patch-clamp amplifier and were digitized and stored on a VCR. All data were filtered (1000 Hz) and analyzed off-line on an IBM-AT computer.

Seal resistances from 1 to 20 GΩ could be obtained in all preparations, but with varying success rates. In the liver cell nuclei about 50% of the attempts to patch were successful, compared to 20% for the other preparations. Because the oocyte, zygote, and embryonic nuclei were extracted by micromanipulation, their surfaces may be less clean than liver nuclei, accounting for the lower success rate of seals.

For germinal vesicles, pronuclei, and two-cell embryo nuclei, we embedded whole cells for electron microscopy (EM) because of the technical difficulties associated with isolating a large number of nuclei. For liver we embedded cell-free nuclei. All samples were prepared identically for EM as follows: cells or nuclei were sedimented and the pellets were fixed with 1% glutaraldehyde and 1% tannic acid in the bath solution (*see above*). Specimens were post-fixed in osmium tetroxide, dehydrated in a graded series of ethanol, and embedded in Medcast-Araldite resin (Ted Pella, Tustin, CA). Uniform silver-gray sections, 40–50 nm thick, were mounted on formvar-coated, carbon-stabilized copper grids, stained with uranyl acetate and Reynolds lead citrate, and examined at 80 kV in a JEOL CX electron microscope.

Results

Ion Channels in Nuclear Envelopes Are Widespread

The zygote serves as a useful model because the cell-free nuclei are viable. Figure 1 shows examples of the dominate states of the pronuclear channel. These data are from different patches clamped to the same pipette potentials (V_p). The high-conductance, nonrectifying channel (left) changes into the low-conductance, rectifying channel (right) in virtually every patch, supporting the assertion that the two conductances are different states of the same channel.

In the present study we compare the nuclei of four different cell types in a developmental sequence: (*a*) the unfertilized oocyte, (*b*) the zygote, (*c*) the two-cell embryo, and (*d*) the adult liver cell. Figure 2 shows light micrographs of these preparations. The nuclei of these cells, which are visible in each micrograph, were removed by micromanipulation in *a–c* and by homogenization and centrifugation in *d*.

Figure 3 presents sample data from the four nuclear preparations. Examples of single-channel recordings are on the left, and the corresponding amplitude histograms are on the right. Each of the samples and the matching histograms result from a step potential, $V_p = 0$ to -25 mV, applied to the patch electrode. We only analyzed patches that contained clear openings and closings, and for which the current flowed equally well in both the inward and the outward direction, as in the example in Fig. 1 (left). Thus we excluded the partially open, rectifying channels shown in Fig. 1 (right). The figure illustrates several discrete current levels at the same voltage. Because some of the levels are difficult to distinguish, we calculate the current-voltage relations using the peak values of the histograms to define the current levels. Thus, in the germinal vesicle and in the two-cell embryo nucleus, we can easily identify two levels of outward current. In the pronucleus, however, it is nearly impossible to recognize

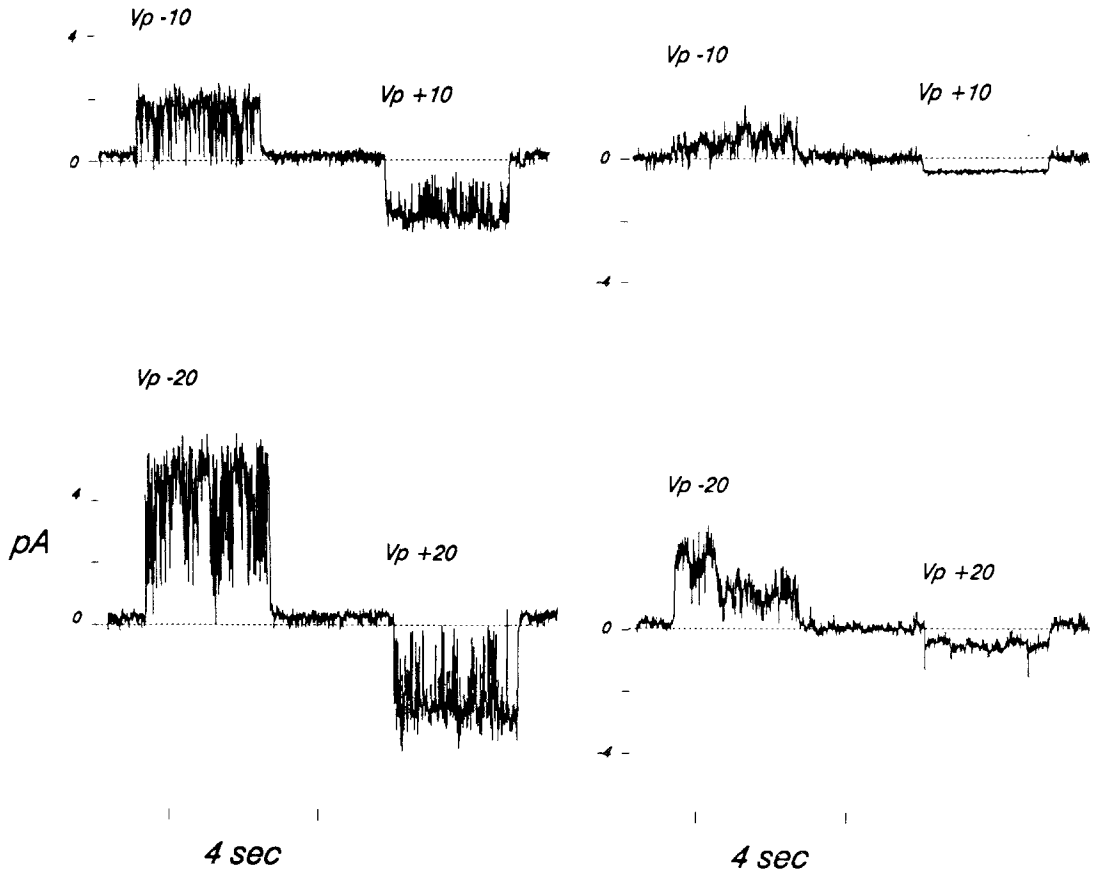

Fig. 1. States of the pronuclear channel at $V_p = \pm 10$ and ± 20 mV. The patches represented on the left (about 10% of the cases) conduct almost equally well in the outward (up) and inward directions. The patches represented on the right (80% of the cases) conduct outward current through a partially open channel and conduct less inward current. In the remaining 10% of the patches on pronuclei, no channels are present

distinct levels because of the extensive flickering (rapid opening and closing) of the channel. The histogram of the pronucleus current data does reveal a second peak, which we use in the current-voltage plots. In the liver nucleus, four well-resolved current levels appear in both the raw data and in the histogram.

Figure 3 shows the general pattern: patches formed on the surface of nuclei from undifferentiated cells (germinal vesicles, pronuclei, and two-cell embryo nuclei) consistently express only one or two peaks in the current amplitude histograms (eight experiments). In contrast, the same size patches on adult liver cell nuclei contain no less than two levels of current (11 experiments), and one patch included seven levels.

The current-voltage relationships in Fig. 4 are constructed from the histograms. Preparations *a*, *b*, and *c* have a nuclear membrane potential, V_{nu}, close to -10 mV (nucleoplasm with respect to cytoplasm; Mazzanti et al., 1990), whereas liver cell nuclei have a membrane potential close to zero. This difference may be due to the harsh treatment of the liver nuclei during isolation, which may influence the membrane potential. In addition the measurements of resting potential from nuclei obtained by micromanipulation were made immediately after enucleation; however, these potentials eventually run down. The measurements on liver cell nuclei are performed approximately 1 hr after isolation. To compare the conductance of channels in diverse nuclei prepared with different techniques, it is therefore convenient to plot current *versus* pipette potential, V_p, rather than current *versus* absolute potential $V = (V_{nu} - V_p)$. Assuming a nominal value of $V_{nu} = -10$ mV for (*a–c*) and $V_{nu} = 0$ mV for (*d*), the $i(V)$ curves would have positive slopes, and they would all reverse near -10 mV. The convention we use results in $i(V_p)$ curves with negative slopes that contain the required information about the patch conductance. We observe a repeating unitary conductance in the range 200–240 pS in all but the blastomere. The peak at

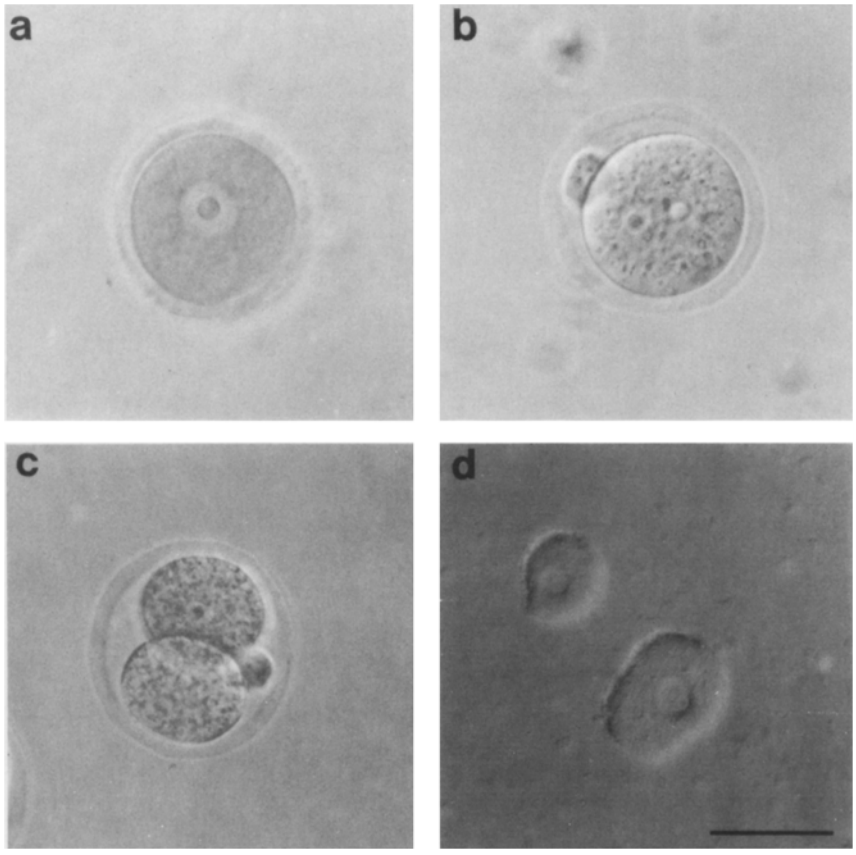

Fig. 2. Four murine preparations used in our experiments: (*a*) unfertilized oocyte, (*b*) zygote, (*c*) two-cell embryo, and (*d*) adult liver cells. The bar on the lower right is 50 μm

300 pS in the two-cell embryo nucleus is probably a mixture of the unitary conductance and substates of unitary conductances. Liver cell nuclei contain the highest number of repeating unitary conductances.

Density of Pores in the Nuclear Envelope

To compare the morphology of the nuclear envelope in the four different preparations, we examined each by electron microscopy. Figure 5 contains samples of representative thin-section images of nuclear envelopes from: (*a*) a germinal vesicle, (*b*) a pronucleus, (*c*) a two-cell embryo nucleus, and (*d*) an adult liver nucleus. The nuclear pore complexes have diameters in the range 75 to 100 nm, in agreement with other studies and consistent with the expected variation in thin-section planes (Unwin & Milligan, 1982; Akey, 1989). We found no correlation between pore diameter and developmental stage of the nucleus. However, we did find a correlation between pore density and developmental stage. To estimate the pore density, we used images like the one shown in Fig. 5. In 5 germinal vesicle envelopes, we measured on average of 3.1 $\pm$ 0.4 pores/μm; 7 pronuclei gave 2.9 $\pm$ 0.6 pores/μm; 4 two-cell embryo stage nuclei gave 5.0 $\pm$ 1.6 pores/μm; and 10 liver nuclei gave 9.1 $\pm$ 2.0 pores/μm. Squaring these values gives a rough estimate of density. Shrinkage during fixation would cause a systematic error in these numbers. Freeze etching is the most quantitative method to measure density (Maul, 1977), and Kartenbeck et al. (1971) compared the values they obtained in rat hepatocytes using both transmission EM and freeze etching. They found that the density of pores in thin section is larger than the density of pore in freeze etch. Thus our technique probably overestimates the density of nuclear pores by at least a factor of eight. We may conclude from our measurements that the relative number of nuclear pores per unit area increases approximately ninefold from oocytes to adult liver cells, but we make no assertions about the absolute number of these pores.

Substates

A comparison of the electrophysiological and the morphological results suggests a connection between the number of conductance levels and the

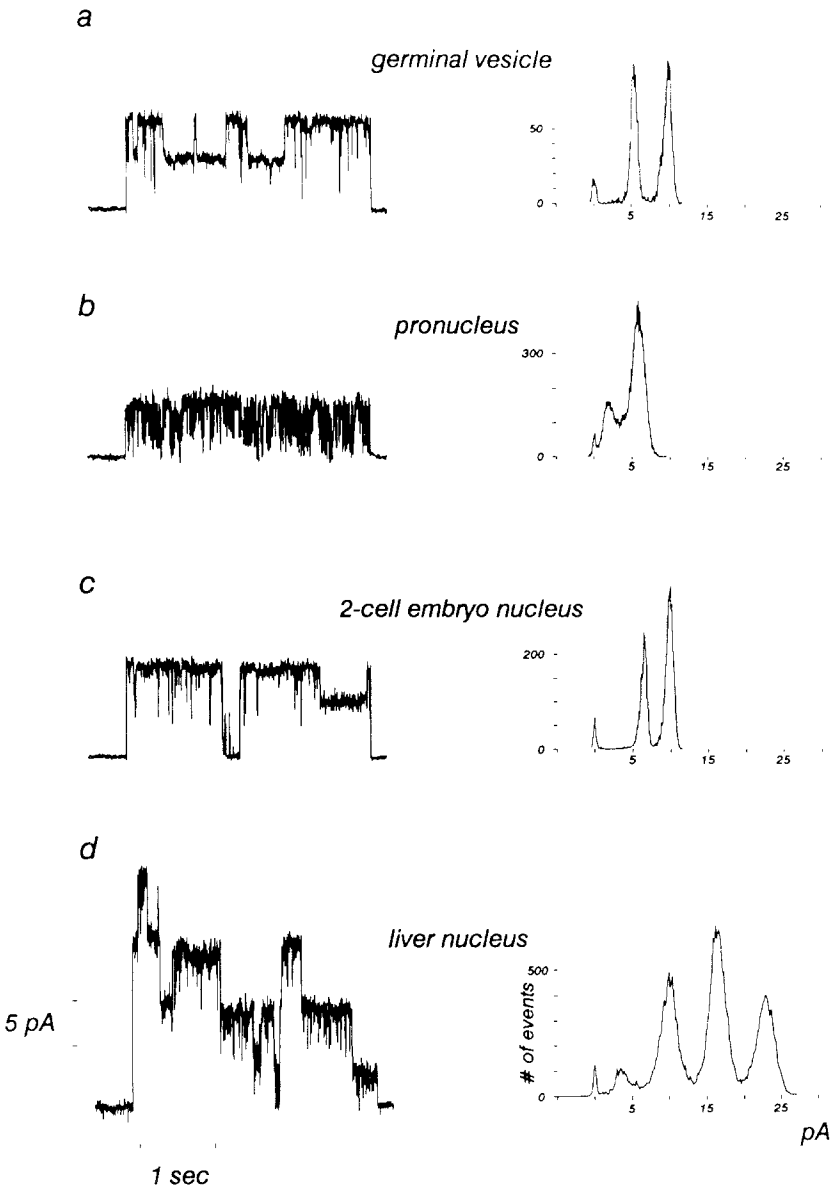

Fig. 3. Presence of a large conductance channel in (*a*) germinal vesicles from oocyte, (*b*) pronuclei from zygotes, (*c*) nuclei from two-cell embryos, and (*d*) liver cell nuclei. On the left are single-channel currents elicited by −25-mV voltage steps applied to the patch pipette. On the right are amplitude histograms obtained from the experiments on the left

number of pores in a patch. In general different conductance levels may result from separate ionic pathways or substates of the same pathway. Examination of the raw data indicates that substates obviously exist to a greater degree than indicated by histogram analysis. To illustrate, Fig. 6 is a sample of raw data from experiments on pronuclei, displayed on an expanded time scale. The three traces on the left were selected to show possible sublevels of the prominent 200-pS state that dominated this particular patch (*cf.* Fig. 1, left). The top line, defined by the largest peak in the amplitude histogram (Fig. 3*b*), corresponds to the 200-pS conductance. The line below it, though it lies on an obvious subconductance level, is close to but does not exactly coincide with the 55-pS conductance. This illustrates that peaks in the histogram and levels in the raw data are not necessarily identical, since the histograms tabulate not only amplitude but kinetics. Conspicuous levels that appear infrequently are lost, and closely adjacent levels merge. To emphasize this point, consider the data in the right-hand column in Fig. 6. These experiments are from three different pronuclei, and they are typical of the partially closed conductance state illustrated in Fig. 1 (right). The two closely apposed dotted lines indicate a conductance substate with approximately one-eighth the value of the 200-pS state. This small state and others like it are not resolved in the amplitude histograms.

Figures 7 and 8 analyze possible substates in liver cell nuclei. Figure 7 shows currents at 10 different voltages and plots the matching current-voltage

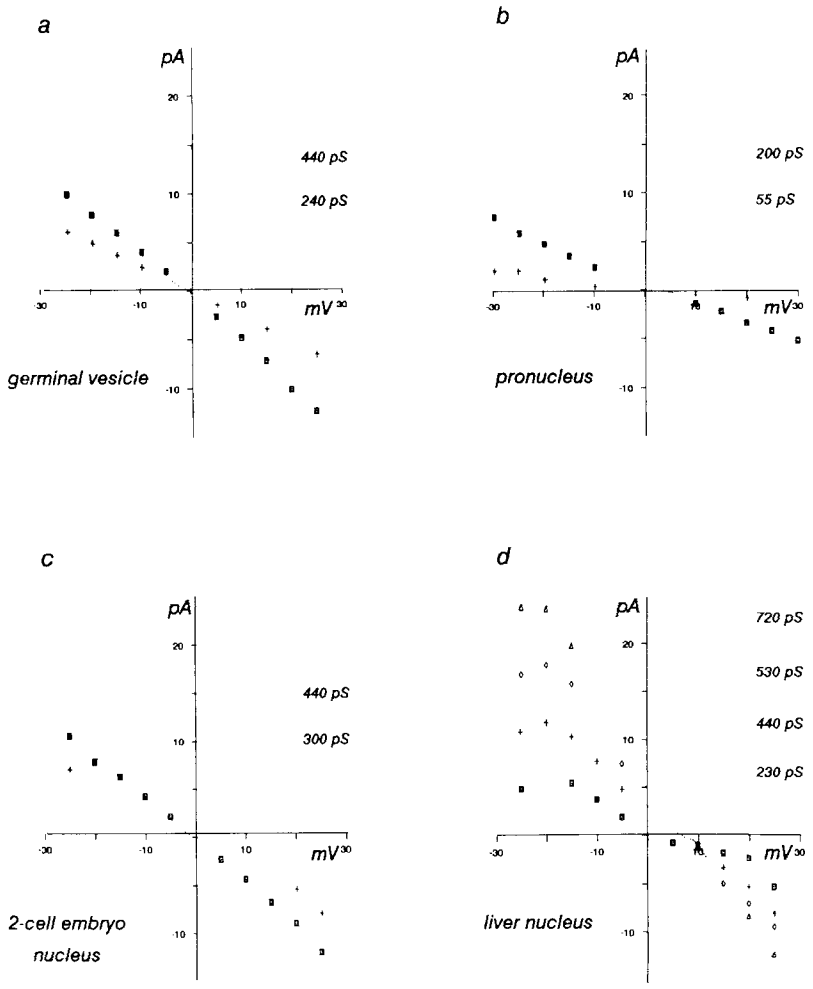

Fig. 4. Current-voltage relations obtained by plotting the peaks of amplitude histograms at 10 different patch potentials from the experiments of Fig. 3. In each panel, the voltage axis is V_p, the potential applied to the patch pipette. The current axis indicates the major peaks in the histograms. The conductance inferred in each graph is from a straight line drawn freehand through the experimental points

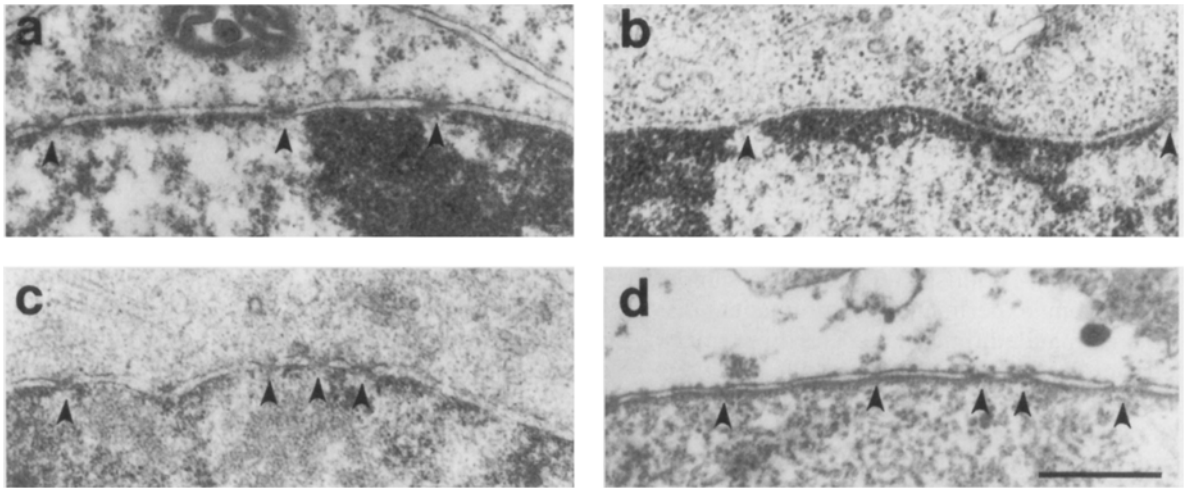

Fig. 5. Electron microscopy of the nuclear membrane of (*a*) a germinal vesicle, (*b*) a pronucleus, (*c*) a two-day embryo nucleus, and (*d*) a liver cell nucleus. The cytoplasmic side is on the top of each micrograph. The arrows indicate nuclear pores whose amplitudes range from 75 to 100 nm. The bar in the lower right is 500 nm

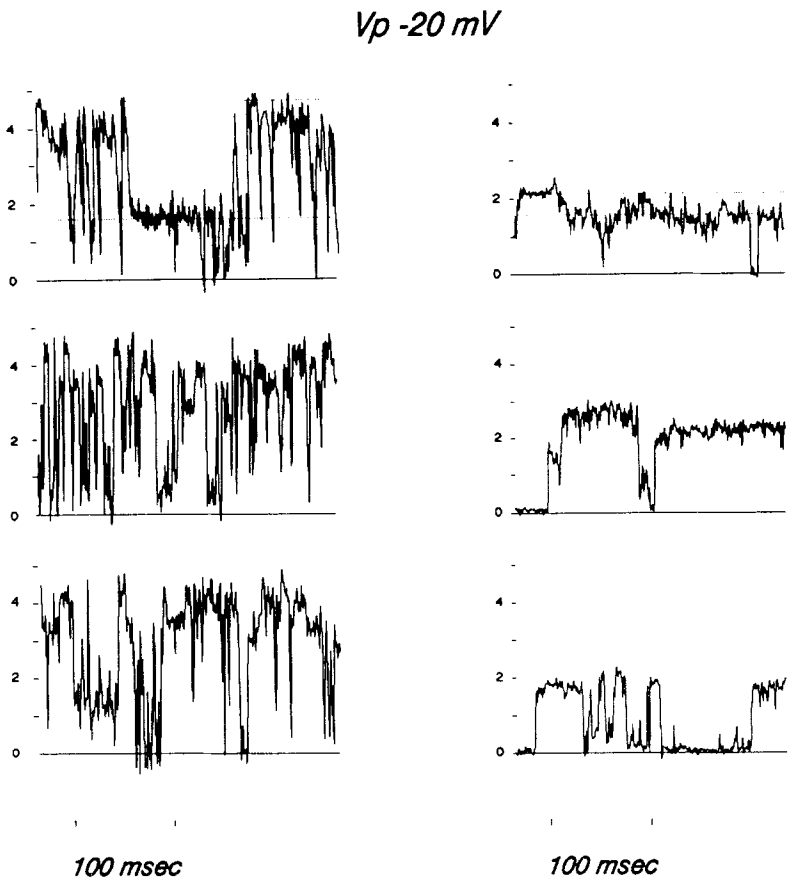

Fig. 6. Presence of sublevels in pronuclei channels. On the left are data from a fully open channel in the pronucleus, in which it is possible to distinguish subconductances. The dotted lines in the top left depict a sublevel (lower) of the 200-pS state (higher). On the right are three separate experiments on the partially open channel. The dotted lines in the top right delineate the smallest observable sublevel, which is approximately one-eighth the amplitude of the 200-pS state

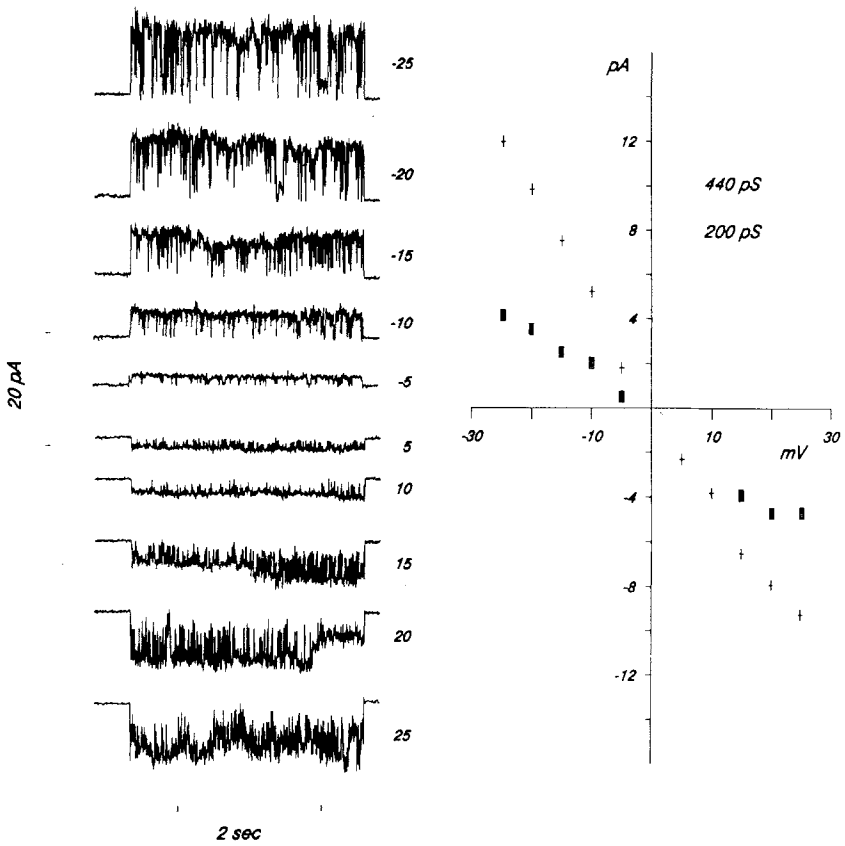

Fig. 7. Presence of sublevels in liver cell nuclei channels. We obtained the data on the left by applying voltage steps to the patch pipette (patch voltage next to the traces). An amplitude histogram analysis of 8 sec of data at each potential gave two major current peaks, which we used to plot the current-voltage relations on the right. The voltage axis is the pipette potential. The two lines represent the conductances indicated in the graphs

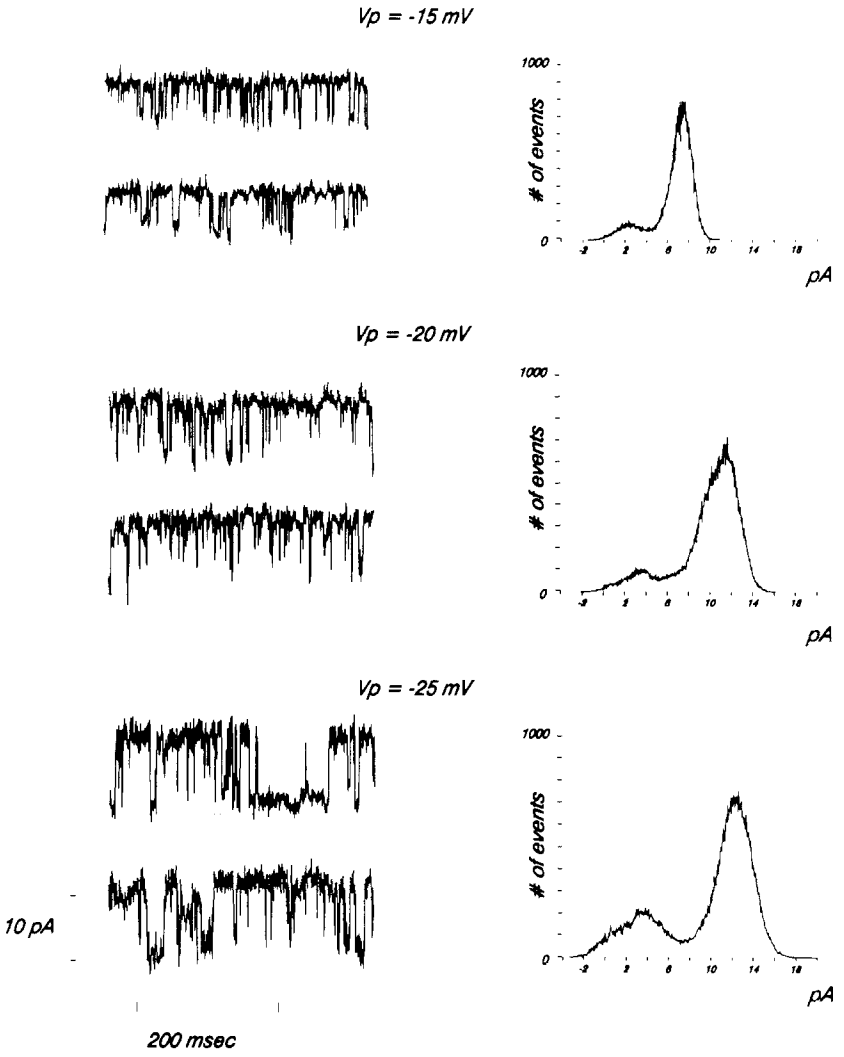

Fig. 8. Two current traces (left) at three different V_ps from the experiment of Fig. 7, plotted on a faster time scale. On the right are amplitude histograms with two clear peaks. The peaks are skewed, indicating the presence of unresolved subconductance levels

relationships, which were derived from histograms. This experiment contains only two separate lines of conductance, as defined by histogram peaks, which is the minimum number for liver cell nuclei. These conductances (200 and 440 pS) closely parallel those in the experiment in Fig. 5*d*. Figure 8 shows the histograms at $V_p = -15$, -20, and -25 mV. The sample data on the left show a complex pattern of levels that emerge as two peaks in the histogram analysis. Thus we conclude that the histogram peaks are obviously composites of a more intricate structure that is not resolved by the present methods.

One complicating feature of the nuclear channel is the relationship between the levels of current that are evident in the raw data and the peaks that appear in the amplitude histograms. From a visual analysis of the traces numerous sublevels are obvious (Fig. 6), but only two peaks appear in the histograms (Fig. 4*b*). The larger peak that defines the 200-pS conductance agrees with the maximum current level in the unprocessed data, but the lower peak at 55 pS is obviously a composite of many smaller states. Indeed, we should expect that even the 200-pS conductance is not a pure state, for closely adjacent levels will always appear as one. Nonetheless we designate the peaks in the histograms as the defining feature of the patch conductance. When the levels are well resolved, as in Fig. 3*d*, the peaks match the single-channel records. When they are not, as in Fig. 8, the peaks provide us with an objective measure of comparison, but they are not easily identified with elementary conductance levels.

Discussion

The Location of the Nuclear Channel

In the cell two phospholipid bilayers envelop the nucleus, the inner membrane, which confines the nuclear material, and the outer membrane, which

extends into the cytoplasm as the rough endoplasmic reticulum (ER). The space between the inner and outer membranes is continuous with the ER lumen. The double-bilayer structure surrounding the nucleus, along with the interruptions in this structure formed by the nuclear pores, are cumulatively referred to as the nuclear envelope. Extranuclear membranes of the intact cell are most likely lost during our isolation procedures (*see* Materials and Methods). Under this assumption the electrode we press to the visible surface of the nucleus forms a patch on the outer membrane of the nuclear envelope.

Nuclear pores are the only structures that span the double bilayer, and they establish a direct connection between the nucleoplasm and the cytoplasm. Because nuclear pore density is high, the patch we form on the outer membrane is likely to contain them. Since these patches also contain K-selective channels, we are led to ask whether the channels and the pores are the same entity.

This question challenges the traditional view of nuclear pores; however, the elaborate structure of pores (Akey et al., 1989; Reichelt et al., 1990) may be compatible with the idea that at least part of the complex can discriminate between ions. If nuclear pores are K selective, then it is the pores themselves that maintain the steady potential of the nucleoplasm. If they are not ion selective, the pores must be closed: open pores would act as a shunt, and ion-selective channels would be impossible to measure, and open pores could not maintain a potential difference. Thus if the nuclear pore complex—or any part of it—is a large, patent canal for the transport of macromolecules, either none occur in our patches (which is unlikely) or they are occluded under our conditions. Another possibility is that the K-selective channels exist as separate integral membrane proteins in the outer membrane. If the K-selective channels are in the outer membrane, and if the inner membrane also contains ionic pathways, the circuit to the nucleoplasm would be complete. But this model, too, would require that the pores in the patch are closed. Other situations may explain the observed electrical connection between the patch solution, the nucleoplasm, and the bath. In the following discussion we refer to the investigated conductance states as nuclear channels, leaving open the question of their exact location.

The Unitary Conductance of the Nuclear Channel

The measurement of 200 pS for the unitary conductance of a fully open channel in the pronucleus is an approximation. Because of substates, patches that contain more than one of these units may show values that are near but are not exact multiples of 200 pS. Thus we interpret 440 pS as the sum of two units (Fig. 4). The higher values of conductance found in liver nuclei, 530 and 720 pS, may be multiples of the basic unit shifted downward by the contributions of underlying conductances.

In all but the pronucleus, the transitions between major conductance levels are infrequent. This visual observation is reflected in the valleys of the histograms, which never reach zero in Fig. 3*b* but nearly do in *a–c*. However, Figs. 7 and 8 from liver nuclei indicate that here, too, assorted modes of conductance substates and flickering may exist.

Our interpretation is that essentially the same channel exists in all preparations, with relative deviations in channel substates and kinetics accounting for the variability in total conductance.

This view leads to the hypothesis that the unitary channel we first observed in the pronucleus is repeated in the other preparations. In the pronucleus the 200-pS state is rare, and when the state is present it is unstable. In the other preparations the 200-pS state is common, and it is therefore the basic unit of the total conductance. However, the total conductance is not an independent sum of identical elements, and the distribution of amplitudes suggests an interdependence between the underlying units.

Nuclear Channels and Nuclear Pores are Correlated

According to Maul (1977) and Gros, Sauvignon and Challice (1980), nuclei from more active cells have the greatest density of pores. This also seems to be the case in our experiments. Hepatocytes have approximately nine times the density of nuclear pores compared to oocytes. Coincidently, hepatocytes also have the greatest number of unitary conductance states per patch. If each of these elementary states represents a pore, it would seem that the patch-clamp method greatly underestimates their density. Taking into account the uncertainties delineated in the Results, EM predicts roughly 10 pores per μm^2 in hepatocytes, or as many as 70 pores per patch. The EM may not, however, represent the number of functional pores in a patch, and disruption may also occur during the patch procedure itself. The methods used for EM and for electrophysiology were the same for all preparations. Thus we conclude only that nuclei with more pores per unit area generally have more channels per patch, without regard to absolute numbers. We also provide evidence for the commonalty of the channel we first reported in the pronucleus.

Similarity to other intracellular membrane chan-

nels exists. The channel in the nuclear envelope is parallel in some respects to a channel in the sarcoplasmic reticulum (SR), first studied in reconstitution experiments (Coronado, Rosenberg & Miller, 1980). Using the patch-clamp technique on a skinned muscle fiber preparation, Tang, Wang and Eisenberg (1989) report that the SR channel is present in about 25% of the patches. The SR channel has a mean open time of several seconds, at least two conductance states, and its maximum conductance is 200 pS with 480 mM K in the patch pipette and in the bath solution. The SR channel in neutral bilayers has a conductance of about 100 pS in symmetric solutions of 120 mM K. The conditions of the experiments are different, and we may not conclude that the nuclear channel and the SR channel are related. Nevertheless, the outer membrane of the nucleus is continuous with the sarcoplasmic reticulum, and it is tempting to postulate some relationship between the two channels. A patch-clamp study of mitochondrial membranes (Sorgato, Keller & Stuhmer, 1987) revealed a slightly anion-selective channel on the inner membrane with a conductance near 100 pS in symmetric 120 mM K. The outer membrane contains 350-pS channels in symmetric 150 mM K.

Role of the Nuclear Channels

What could be the function of ion channels in the nuclear membrane? In smooth muscle cells and in rat liver nuclei (Williams et al., 1985; Nicotera et al., 1989) the nuclear membrane appears to be involved in the regulation of calcium. In pronuclei (Mazzanti et al., 1990), we have shown previously that the nuclear resting potential is influenced by external (cytoplasmic) potassium. These results imply the existence of an ion-selective pathway across the nuclear envelope. One function of the pronuclear channel, which appears to have K selectivity, could be to help maintain the nuclear resting potential. As we argued above, if the channels we observed are not the pores, the existence of relatively low conductance, ion-selective channels in parallel with free-diffusion nuclear pores is paradoxical. If the channels we describe are the pores, the conductance of 200 pS is smaller than would be expected from the structure of the pore. Regardless of their identity, the number of channels and the number of pores seem to parallel one another in the four preparations we studied. Since one function of nuclear pores is to transport macromolecules, pores may incorporate ion-selective channels in their infrastructure to balance the charge carried by macromolecules as they move across the nuclear envelope.

The authors wish to thank R.L. DeHaan and W. Sale for a critical reading of the manuscript. We also wish to recognize Ms. B.J. Duke for preparing solutions and Mr. W.N. Goolsby for designing, building, and maintaining the electronics and computer facilities necessary for this work. This work was supported by National Institutes of Health HL-27385.

References

Akey, C.W. 1989. Interaction and structure of the nuclear pore complex revealed by cryo-electron microscopy. *J. Cell Biol.* **109:**955–970

Blobel, G., Potter, V.R. 1966. Nuclei from rat liver: Isolation method that combines purity with high yield. *Science* **154:**1662–1665

Coronado, R., Rosenberg, R.L., Miller, C. 1980. Ionic selectivity, saturation, and block in a K-selective channel from sarcoplasmic reticulum. *J. Gen. Physiol.* **76:**425–445

Dingwall, C., Laskey, R.A. 1986. Protein import into the cell nucleus. *Annu. Rev. Cell Biol.* **2:**367–390

Gerace, L. 1988. Functional organization of the nuclear envelope. *Annu. Rev. Cell Biol.* **4:**335–374

Gros, D., Sauvignon, M., Challice, C.E. 1980. Changes in nuclear pore density of myocardial cells during differentiation. *IRCS Med. Sci.* **8:**744

Ito, S., Loewenstein, W.R. 1965. Permeability of a nuclear membrane: Changes during normal development and changes induced by growth hormone. *Science* **150:**909–910

Kartenbeck, J., Zentgraf, H., Schhr, U., Franke, W.W. 1971. The nuclear envelope in freeze-etching. *Adv. Anat. Embryol. Cell Biol.* **45:**1–55

Loewenstein, W.R., Kanno, Y. 1963. Some electrical properties of a nuclear membrane examined with a microelectrode. *J. Gen. Physiol.* **46:**1123–1140

Maul, G.G. 1977. The nuclear and cytoplasmic pore complex: Structure, dynamics, distribution, and evolution. *Int. Rev. Cytol.* **6(Suppl.):**75–186

Mazzanti, M., DeFelice, L.J. 1987. Na channel kinetics during the spontaneous heart beat in embryonic chick ventricle cells. *Biophys. J.* **52:**95–100

Mazzanti, M., DeFelice, L.J., Cohen, J., Malter, H. 1990. Ion channels in the nuclear envelope. *Nature* **343:**764–767

McGrath, J., Solter, D. 1983. Nuclear transplantation in the mouse embryo by microsurgery and cell fusion. *Science* **220:**1300–1302

Newport, J.W., Forbes, D.J. 1987. The nucleus: Structure, function and dynamics. *Annu. Rev. Biochem.* **56:**535–565

Nicotera, P., McConkey, P., Jones, D.P., Orrenius, S. 1989. ATP stimulates Ca uptake and increases the free Ca concentration in isolated rat liver nuclei. *Proc. Natl. Acad. Sci. USA* **86:**453–457

Reichelt, R., Holzemburg, A., Buhle, E.L., Jr., Jarnik, M., Engle, A., Aebi, U. 1990. Correlation between structure and mass distribution of the nuclear pore complex and distinct pore complex components. *J. Cell Biol.* **110:**883–894

Sorgato, M.C., Keller, B.U., Stuhmer, W. 1987. Patch-clamping of the inner mitochondrial membrane reveals a voltage-dependent ion channel. *Nature* **330:**498–500

Tang, J.M., Wang, J., Eisenberg, R.S. 1989. K-selective channel from sarcoplasmic reticulum of split lobster muscle fibers. *J. Gen. Physiol.* **94:**261–278

Unwin, P.N.T., Milligan, R.A. 1982. A large particle associated with the perimeter of the nuclear pore complex. *J. Cell Biol.* **93:**63–75

Williams, D.A., Fogarty, K.E., Tsien, R.Y., Fay, F.S. 1985. Ca gradients in single smooth muscle cells revealed by the digital imaging microscope using Fura-2. *Nature* **318:**558–561

Received 18 September 1990; revised 13 November 1990